OPEN

PRS GLOBAL OPEN

ORIGINAL ARTICLE

Pediatric/Craniofacial

Computational Analysis of the Mature Unilateral Cleft Lip Nasal Deformity on Nasal Patency

Dennis O. Frank-Ito, PhD*†‡
David J. Carpenter, BS, MHS*§
Tracy Cheng, AB*§
Yash J. Avashia, MD¶
David A. Brown, MD, PhD¶
Adam Glener, MD¶
Alexander Allori, MD, MPH¶
Jeffrey R. Marcus, MD¶

Background: Nasal airway obstruction (NAO) due to nasal anatomic deformities is known to be more common among cleft patients than the general population, yet information is lacking regarding severity and variability of cleft-associated nasal obstruction relative to other conditions causing NAO. This preliminary study compares differences in NAO experienced by unilateral cleft lip nasal deformity (uCLND) subjects with noncleft subjects experiencing NAO.

Methods: Computational modeling techniques based on patient-specific computed tomography images were used to quantify the nasal airway anatomy and airflow dynamics in 21 subjects: 5 healthy normal subjects; 8 noncleft NAO subjects; and 8 uCLND subjects. Outcomes reported include Nasal Obstruction Symptom Evaluation (NOSE) scores, cross-sectional area, and nasal resistance.

Results: uCLND subjects had significantly larger cross-sectional area differences between the left and right nasal cavities at multiple cross sections compared with normal and NAO subjects. Median and interquartile range (IQR) NOSE scores between NAO and uCLND were 75 (IQR = 22.5) and 67.5 (IQR = 30), respectively. Airflow partition difference between both cavities were: median = 9.4%, IQR = 10.9% (normal); median = 31.9%, IQR = 25.0% (NAO); and median = 29.9%, IQR = 44.1% (uCLND). Median nasal resistance difference between left and right nasal cavities were 0.01 pa.s/ml (IQR = 0.03 pa.s/ml) for normal, 0.09 pa.s/ml (IQR = 0.16 pa.s/ml) for NAO and 0.08 pa.s/ml (IQR = 0.25 pa.s/ml) for uCLND subjects.

Conclusions: uCLND subjects demonstrated significant asymmetry between both sides of the nasal cavity. Furthermore, there exists substantial disproportionality in flow partition difference and resistance difference between cleft and noncleft sides among uCLND subjects, suggesting that both sides may be dysfunctional.
(Plast Reconstr Surg Glob Open 2019;7:e2244; doi: 10.1097/GOX.0000000000002244; Published online 16 May 2019.)

*From the *Division of Head and Neck Surgery and Communication Sciences, Duke University Medical Center, Durham, N.C.; †Computational Biology and Bioinformatics PhD Program, Duke University, Durham, N.C.; ‡Department of Mechanical Engineering and Materials Science, Duke University, Durham, N.C.; §Duke University School of Medicine, Durham, N.C.; and ¶Division of Plastic, Maxillofacial and Oral Surgery, Duke University Medical Center, Durham, N.C.*

Supported the National Institutes of Health under Award Numbers T32DC013018-03 and R01DE028554-01.

Received for publication February 20, 2019; accepted March 8, 2019.

DOI: 10.1097/GOX.0000000000002244

INTRODUCTION

The anatomic deformity associated with unilateral cleft lip nasal deformity (uCLND) creates multiple sites of nasal airway obstruction (NAO), such as septal deviation, nostril atresia, valvular stenosis or deficiency, turbinate hypertrophy, and altered nasal floor from deficiency of maxillary growth.[1–6] These deformities impair nasal breathing, which negatively impact patients' quality of life.[1,7–11] Patients with uCLND routinely suffer from sleep-disordered breathing, they snore frequently and experience loud labored breathing during sleep.[12–21] Furthermore, some patients report air hunger and trouble breathing during exercise.[22]

The functional implications of uCLND have been poorly understood and underappreciated.[22] Nonetheless, majority of cleft lip and/or cleft palate studies that have

Disclosure: *The authors have no financial interest to declare in relation to the content of this article. The content is solely the responsibility of the authors and does not represent the official views of the National Institutes of Health.*

addressed NAO have focused on a comparison with normal subjects and/or among different cleft phenotypes.[6–10,22–29] Although these studies have demonstrated the impact of uCLND on nasal breathing difficulty, they do not provide insights into variabilities in nasal dysfunction across cleft and noncleft subjects with NAO. The cleft literature is deficient on information comparing the extent of impaired nasal breathing in cleft-associated nasal obstruction with other conditions associated with nasal obstruction. Quantifiable evidence pertaining to differences in nasal breathing patterns across different disease conditions is important because it will provide the cleft and craniofacial community with objective evidence regarding extent of the effect of uCLND on nasal breathing and provide perspective on the importance of treatment.

Innovative assessment tools to objectively describe NAO may provide enhanced detail for understanding uCLND-associated nasal obstruction. Computational fluid dynamics (CFD) methods have shown significant promise in describing upper airway physiology.[30–35] They allow for the merger of anatomy and physiology by creating anatomically realistic 3-dimensional (3D) nasal cavity models from patient-specific radiographs with computed measures of airflow, heat transfer, and air humidification.[35–41] The purpose of this preliminary study is to use CFD modeling to quantify nasal patency differences associated with nasal obstruction in uCLND patients compared with noncleft patients who had a clinical diagnosis of nonreversible, surgically treatable NAO.

MATERIAL AND METHODS

Selection of Study Cohort

This is a retrospective study approved by the Duke University Health System Institutional Review Board for Clinical Investigations. Twenty-one subjects with high resolution computed tomography (CT) scans were selected based on a chart review of medical records from 2010 to 2017. Selected subjects were classified into 3 groups:

(1) Five subjects (25–70 years, 2 males, and 3 females) with radiographically healthy normal nasal cavity and sinus anatomy (NORMAL). These subjects had no nasal airway functional symptoms.
(2) Eight noncleft subjects (20–55 years, 5 males, and 3 females) with a clinical diagnosis of nonreversible, surgically treatable cause for NAO such as septal deviation, turbinate hypertrophy resistant to medical therapy, and lateral nasal wall collapse (NAO; Table 1).
(3) Eight subjects (15–35 years, 2 males, and 6 females) with a clinical diagnosis of uCLND and have not had definitive cleft rhinoplasty or septoplasty for correction of NAO (CLEFT; Table 1).

Nasal Airway Reconstruction

Subject-specific and anatomically realistic 3D nasal cavity models were created from radiographic images of CT scans for all subjects. Nasal cavity models were segmented, from CT to create 3D nasal models, similar to previously published models by our group.[33,34,37,39,40,42–44] Next, 3D nasal cavity models were imported into the mesh-generating software, ICEM-CFD 16.1 (ANSYS, Inc., Canonsburg, Pa.) for creation of planar inlet surface at the nostrils, a 2-cm tube attached to the nasopharynx, and an outlet surface at the lower end of the tube. To solve the discretized governing equations of fluid flow, each nasal cavity model was discretized by generating approximately 4 million tetrahedral mesh elements inside the airway based on a mesh density refinement analysis study in Frank-Ito et al.[40]

Nasal Airflow Simulations

Following discretization of nasal models, the CFD software package Fluent 16.1 (ANSYS, Inc., Canonsburg, Pa.)

Table 1 : Basic Demographic Information and Diagnoses

NAO Subjects				CLEFT Subjects			
Gender	**Race**	**Age**	**Diagnosis**	**Gender**	**Race**	**Age**	**Cleft Type**
Male	White	37	Deviated nasal septum External nasal deformity	Female	White	15	Unilateral completed cleft lip alveolus and palate (Veau 3)
Female	White	27	Deviated nasal septum External nasal deformity Inferior turbinate hypertrophy	Male	African American	15	Unilateral complete cleft lip alveolus
Male	White	33	Deviated nasal septum External nasal deformity Inferior turbinate hypertrophy	Female	African American	15	Unilateral completed cleft lip alveolus and palate (Veau 3)
Female	White	53	Deviated nasal septum Bilateral vestibular stenosis Bilateral inferior turbinate hypertrophy	Female	White	15	Unilateral completed cleft lip alveolus and palate (Veau 3)
Female	White	22	Deviated nasal septum Bilateral vestibular stenosis	Female	White	31	Unilateral completed cleft lip alveolus and palate (Veau 3)
Male	White	38	Deviated nasal septum Inferior turbinate hypertrophy	Female	Hispanic	32	Unilateral completed cleft lip alveolus and palate (Veau 3)
Male	White	46	Deviated nasal septum External nasal deformity Inferior turbinate hypertrophy	Female	White	24	Unilateral incomplete cleft lip
Male	White	44	Deviated nasal septum External nasal deformity Bilateral vestibular stenosis	Male	White	17	Unilateral completed cleft lip alveolus and palate (Veau 3)

was used to conduct steady-state simulations of laminar incompressible inspiratory airflow at resting inhalation rates. ANSYS Fluent uses the finite volume method to numerically solve the discretized Navier–Stokes equations. Because the flow velocities through the nasal passage during low-to-moderate breathing rate usually have a Mach number $\ll 0.2$,[45] the conservation of mass and momentum governing equations for laminar, incompressible steady-state flow reduces to $\nabla \cdot \vec{u} = 0 \;\; \rho(\vec{u} \cdot \nabla)\vec{u} = -\nabla p + \mu \nabla^2 \vec{u}$

where $\vec{u} = \vec{u}(x, y, z)$ is the velocity vector, $\rho = 1.204$ kg/m^3 is fluid density, $\mu = 1.825 \times 10^{-5}$ kg / m – s is dynamic viscosity, and p is pressure. Airflow was simulated in each nasal cavity using these boundary conditions: at the nasal wall, no-slip, and stationary wall; at the inlet, a "pressure-inlet" boundary condition was specified at the inlet surface with gauge pressure set to zero; and a "pressure-outlet" condition at the outlet with a negative gauge pressure set to target resting breathing of 15 l/min flow rate.

Computed Outcomes and Analysis

Analyses of nasal cavity anatomy (shape and size) and airway function (airflow profile) were conducted across the 3 categories of subjects (NORMAL, NAO, and CLEFT). Data computed for outcomes of nasal cavity shape and size included: (1) cross-sectional images of the airway at 11 cross sections from immediately after the posterior end of nostrils tip to choana (Fig. 1); (2) unilateral left–right absolute difference in cross-sectional area at every cross section; and (3) unilateral shape factor circularity at each cross section of the nasal cavity. Shape factor circularity tells the degree to which each unilateral cross section is similar to a circle; it is a measure that describes the form and roughness/irregularity of a shape. Circularity is dimensionless and it is defined as $4\text{pi}A / P^2$, where A is unilateral cross-sectional area of airway at each cross section and P is unilateral cross-sectional perimeter of airway at each cross section. The circularity of a given shape lies between 0 and 1, shapes with smaller circularity values are less round (and/or more irregular) and higher circularity value shapes are more round (and/or less irregular). The circularity of a circle is 1.

Data computed for functional outcomes related to nasal airflow and airway patency included: (1) unilateral airflow partition between both (left and right) sides of the nasal cavity; (2) unilateral nasal resistance; and (3) flow streamline visualization of air in the nasal cavity. Unilateral airflow partition (represented in percent) is defined as unilateral flow rate into a particular side divided by total (bilateral) flow rate. Nasal resistance was calculated as $\Delta P / Q$ (Pa.s/mL) where ΔP is the unilateral pressure drop from nostril to choana, and Q is the unilateral volumetric flow rate. Nasal resistance calculated from nostrils to choana has been reported to capture patients' symptoms of nasal obstruction more accurately than that calculated from nostrils to posterior portion of the nasopharynx.[46] Furthermore, patient-reported Nasal Obstruction Symptom Evaluation

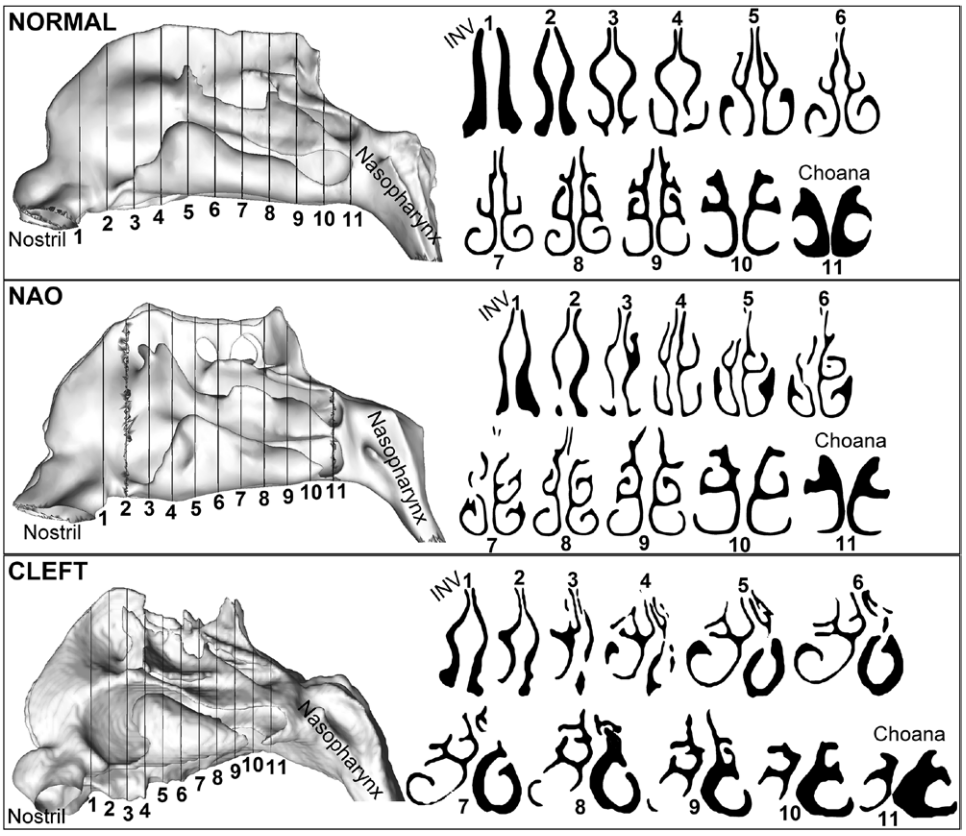

Fig. 1. Cross-sectional images of the nasal cavity at 11 cross sections from posterior end of nostrils tip to choana for NORMAL, NAO, and CLEFT subjects. INV, internal nasal value.[61]

(NOSE) scores for NAO and CLEFT subjects were collected. NOSE is a validated 5-item scale (0: good to 4: bad) with items relating to nasal congestion, blockage, difficulty breathing, trouble sleeping, and air hunger sensation during exercise.

To assess measures of central tendency and dispersion, descriptive statistics such as median and interquartile range (IQR) were reported for computed outcomes due to the relative small patient sample in this study. Furthermore, boxplots and error bar (mean ± SD) charts were constructed for computed outcomes. Analyses were performed using MATLAB R2016a software (MathWorks, Inc, Natick, Mass.).

RESULTS

Nasal Cavity Anatomy

Cross-sectional nasal cavity images of the anatomy at 11 cross sections depicted distinct morphological differences for NORMAL, NAO, and CLEFT subjects (Fig. 1). These anatomical differences in nasal airway were due to CLEFT- and NAO-related pathological deformities compared with those of NORMAL. Furthermore, there was a significant middle-to-posterior septal deviation in the cleft subject from cross section 4 to cross section 11 (choana; Fig. 1).

Figure 2 shows the results of unilateral cross-sectional area differences describing the degree of asymmetry between the left and right sides of the nasal cavity. Mean (± SD) cross-sectional area differences between both unilateral sides across all 11 cross sections ranged from 6.68 ± 6.23 mm2 (at cross section 2) to 28.95 ± 21.483 mm2 (at cross section 5) for NORMAL subjects. The range for NAO subjects was 26.93 ± 24.61 mm2 (at cross section 10) to 54.95 ± 33.12 mm2 (at cross section 2) and 29.18 ± 19.69 mm2 (at cross section 2) to 75.96 ± 54.48 mm2 (at cross section 11) for CLEFT subjects. The degree of asymmetry was the greatest for NAO subjects at the anterior region, and was the greatest at the middle-to-posterior region for CLEFT subjects (Fig. 2). In general, CLEFT subjects consistently demonstrated the highest asymmetry for majority of the cross sections.

As demonstrated in Figure 3A, unilateral circularity for NORMAL subjects ranged from 0.06 ± 0.01 (right-side cross section 7) to 0.70 ± 0.27 (left-side cross section 11). With the exception of cross sections 8, 9, and 10, unilateral circularity values between the left and right nasal cavity were mostly homogenous. Among NAO subjects (Fig. 3B), unilateral circularity ranged from 0.05 ± 0.01 (cross section 7) to 0.52 ± 0.30 (cross section 11) on the less affected side, and from 0.05 ± 0.01 (cross section 5) to 0.55 ± 0.32 (cross section 11) on the more affected side. Unilateral circularity between both sides of the nasal cavity in NAO subjects was very dissimilar at the anterior cross sections (cross sections 1–4) and mostly similar from cross sections 6 to 11. Unilateral circularity among CLEFT subjects ranged from 0.07 ± 0.02 (cross section 6) to 0.28 ± 0.09 (cross section 1) on the noncleft side, and from 0.08 ± 0.02 (cross section 6) to 0.28 ± 0.17 (cross section 1) on the cleft side (Fig. 3C). CLEFT subjects exhibited the greatest dissimilarity in unilateral circularity values between both sides of their nasal cavity; nearly every cross section between the cleft and noncleft sides had sizeable variability.

Nasal Airflow Function

The distribution of airflow streamlines are illustrated in Figure 4. Airflow streamlines in the CLEFT nasal cavity traveled via limited and narrowed pathways due to severe nasal occlusion compared to NORMAL (Fig. 4A), and NAO (Figure 4B). (Plots of airflow streamline patterns in the nasal cavity were based on 50 equally spaced and randomly selected seed points on the nostril surface.)

As depicted in Figure 5A, patient-reported NOSE scores were higher in NAO subjects (median NOSE = 75) compared with CLEFT (median NOSE = 67.5) subjects. However,

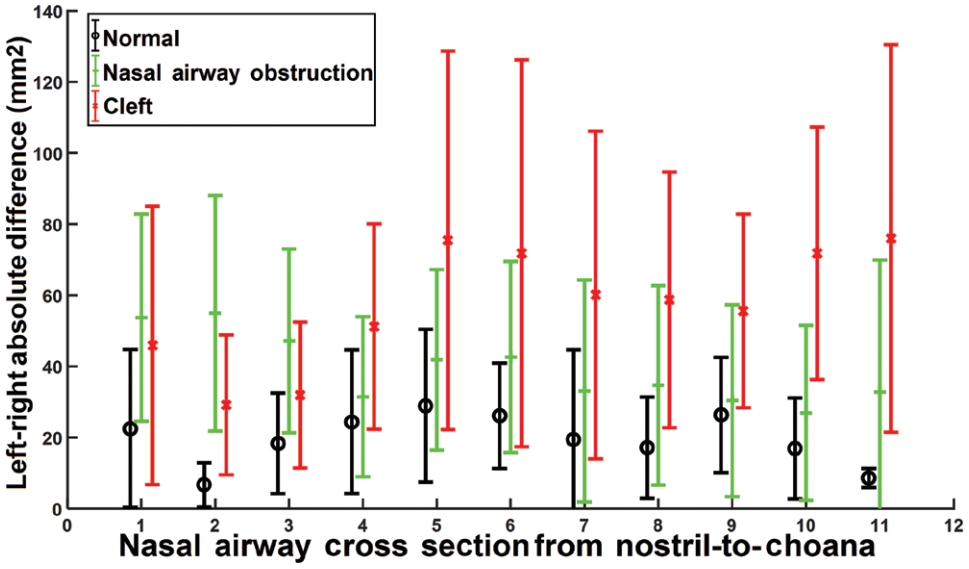

Fig. 2. Absolute unilateral left–right cross-sectional area differences at each cross section for NORMAL, NAO, and CLEFT subjects. Error bar is mean ± SD.

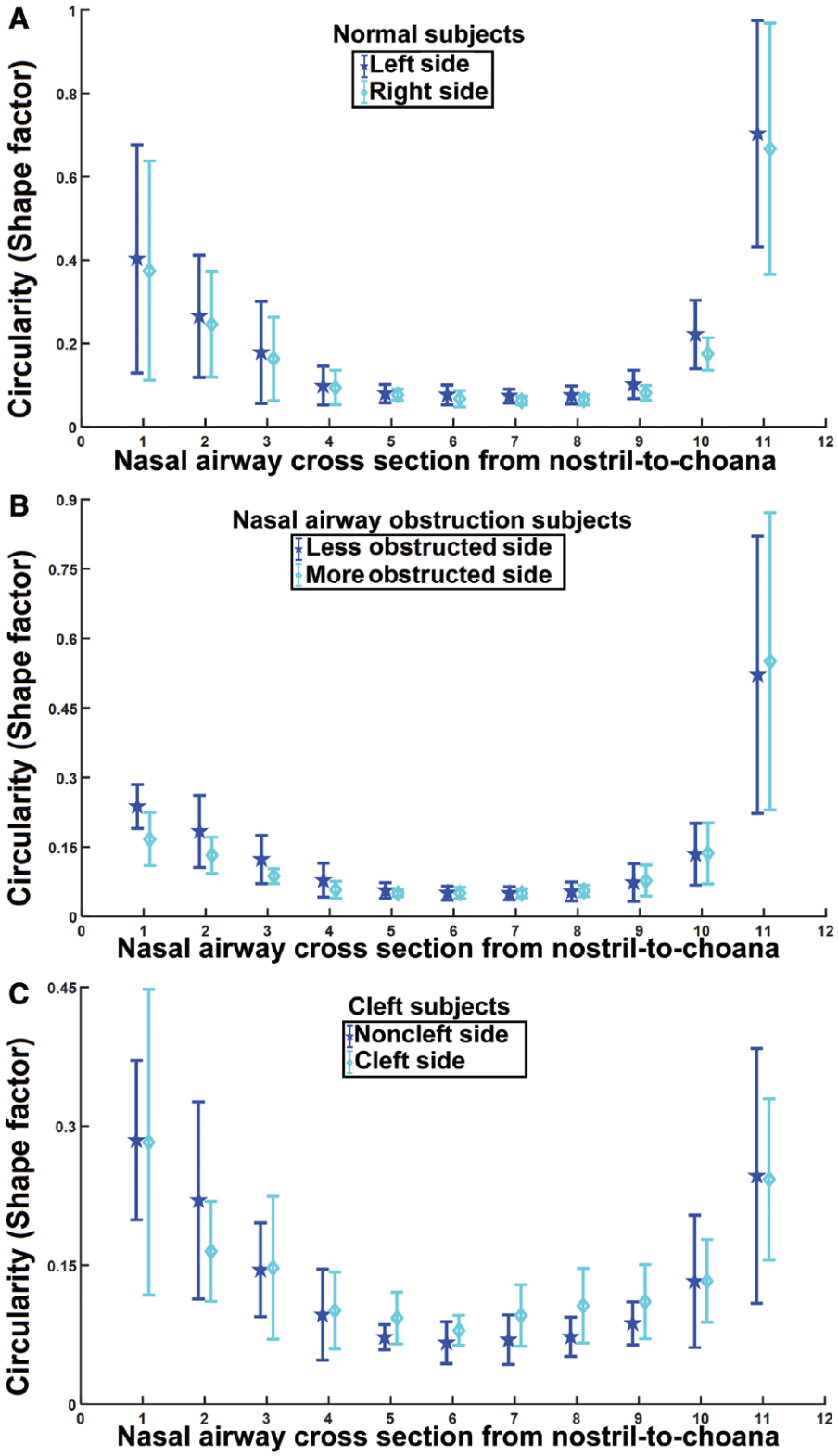

Fig. 3. Unilateral shape factor circularity at each cross section of the nasal cavity for (A) Normal Subjects, (B) NAO Subjects, and (C) CLEFT Subjects.

variability in NOSE scores among CLEFT subjects was 7.5 points higher than in NAO subjects; IQR = 30 for CLEFT versus IQR = 22.5 for NAO. Next, airflow partition results in Figure 5B showed that the predominately affected side (AS) and the less affected side (NS) were considerably different among NAO subjects; median values were

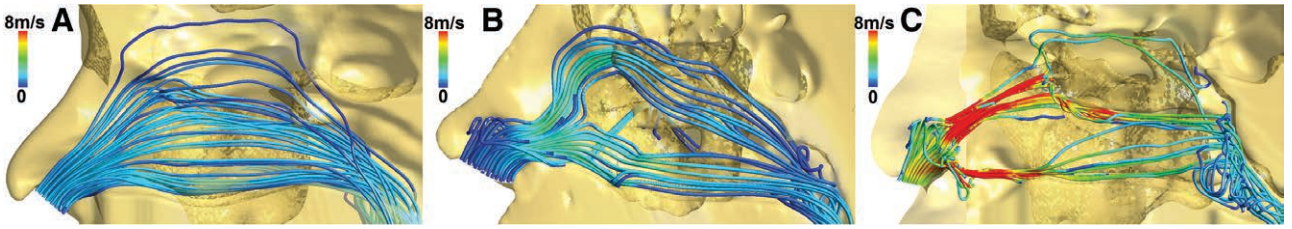

Fig. 4. CFD simulated nasal airflow streamline pattern in (A) NORMAL subject; (B) NAO subject; and (C) CLEFT subject.

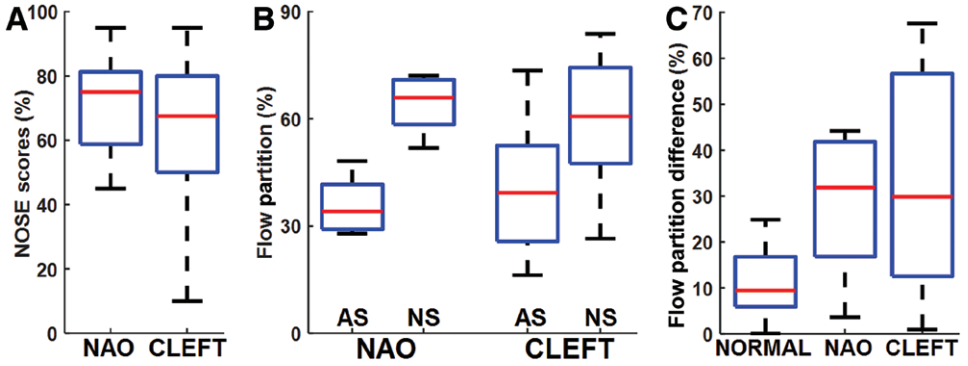

Fig. 5. A, Boxplot comparing NOSE scores between NAO and CLEFT subjects. B, Unilateral airflow partition for both sides of the nasal cavity for NAO and CLEFT subjects. Among CLEFT subjects, AS is the side with unilateral cleft lip deformity and NS is the noncleft side. C, Unilateral airflow partition difference between both sides of the nasal cavity for NORMAL, NAO, and CLEFT subjects. AS, predominately affected side for NAO subjects; NS, less obstructed size.

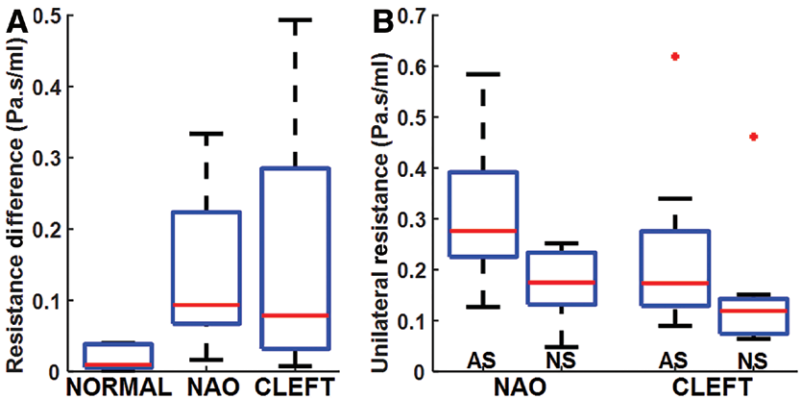

Fig. 6. A, Unilateral nasal resistance difference between both sides of the nasal cavity for NORMAL, NAO, and CLEFT subjects. B, Unilateral nasal resistance for both sides of the nasal cavity for NAO and CLEFT subjects. Among CLEFT subjects, AS is the side with unilateral cleft lip deformity and NS is the noncleft side. AS, predominately affected side for NAO subjects; NS, less obstructed size.

AS = 34.1% versus NS = 65.9%, with a distribution spread of IQR = 12.5%. Among CLEFT subjects, median values were AS = 39.3% versus NS = 60.7%, with a distribution spread of IQR = 26.8%. (Note that the AS for NAO subjects is the more obstructed size, which is also side where the nasal septum is deviated, whereas AS for CLEFT subjects is the side with unilateral cleft lip deformity.) Furthermore, a pairwise comparison of unilateral airflow partition difference between the left and right nasal cavities in Figure 5C indicated that normal subjects had a median difference of 9.4% (IQR = 10.9%), 31.9% (IQR = 25.0%) for NAO subjects, and CLEFT subjects had a median difference of 29.9% (IQR = 44.1%).

Results from Figure 6A revealed that the distribution of unilateral left-to-right difference in nasal resistance was both narrowest and lowest in NORMAL subjects (median = 0.01 pa.s/ml, IQR = 0.03 pa.s/ml), compared with NAO (median = 0.09 pa.s/ml, IQR = 0.16 pa.s/ml) and CLEFT (median = 0.08 pa.s/ml, IQR = 0.25 pa.s/ml), with CLEFT subjects having the largest variability. In addition, as expected, nasal resistance on the AS was higher than on the less affected side (NS) for both NAO and CLEFT

subjects (Fig. 6B). However, median nasal resistance difference between AS (0.28 pa.s/ml) and NS (0.17 pa.s/ml) in NAO subjects was 0.11 pa.s/ml; which is higher than 0.05 pa.s/ml, the median nasal resistance difference between AS (0.17 pa.s/ml) and NS (0.12 pa.s/ml) for CLEFT subjects. Suggesting that unlike in NAO subjects, with an obvious predominantly obstructed side, CLEFT subjects do not exhibit such predominantly obstructed side between AS and NS sides (Fig. 6B).

DISCUSSION

The results of our nasal cavity anatomical comparisons revealed regional cross-sectional airway asymmetry where septal deviation was considerably prominent among the cohort of NAO and CLEFT subjects studied (Fig. 2). The location of deviated nasal septum among NAO subjects was mostly around the anterior to middle portion, whereas CLEFT subjects exhibited greater middle-to-posterior septal deviation in addition to anterior deviation. This finding among cleft subjects is in agreement with reports by Friel et al[25] suggesting that there is a significant degree of deviation at the middle-to-posterior portion of the septum. Nonetheless, surgeries for skeletally mature cleft lip nasal deformity often do not attempt to correct middle-to-posterior septal deviations, corresponding to the osseous septum.[8,9,25] This unrepaired middle-to-posterior deviation accounts for about 75% of the maximal degree of septal deviation within the nasal cavity.[25] Unlike anterior cartilaginous septoplasty, middle-to-posterior osseous septoplasty is relatively more technically challenging to perform and has attendant risks associated with osseous resection, such as mucosal tears, postsurgery bleeding, and cerebrospinal fluid leak.[8,25] However, there is significant deviation around the middle-to-posterior septum that may create residual obstruction after surgery.[25]

As described in Figure 5A, variability in patient-reported NOSE assessment among CLEFT subjects was higher than in NAO subjects. This high variability may allude to the fact that these subjects may be having difficulty self-reporting nasal obstruction symptoms because they have lived without knowing what it is to have normal nasal function.[9,47] Furthermore, for NAO subjects, unilateral flow partition (Fig. 5B) and unilateral resistance (Fig. 6B) between AS and NS were very different. This is in contrast with CLEFT subjects showing a reduced difference between AS and NS, and a high measure of variability based on IQR. This reduced difference in unilateral flow partition and unilateral resistance among CLEFT subjects and high IQR may point to the fact that obstruction on AS may not be dominating the obstruction on NS for CLEFT subjects as was observed in NAO subjects. Rather, CLEFT subjects demonstrated considerable nasal dysfunction on both sides. This finding is consistent with what Shih and Sykes[48] noted, in uCLND the nasal septum is deviated on both sides of the nasal cavity; the septum is deviated to the noncleft side at the anterior portion, and deviated to the cleft side posteriorly.[23,24] In addition, Farzal et al[27] reported no significant difference in unilateral nasal volume between cleft and noncleft sides based on 3D volume quantifications. However, there is disagreement in the literature on the side with greater obstruction as some articles reported differences in unilateral nasal cavity volumes, unilateral cross-sectional areas, and/or unilateral airflow (with the cleft side mostly affected), as measured by radiographic images, acoustic rhinometry, and rhinomanometry.[11,28,29,49,50]

Additionally, Sandham and Solow[49] suggested no significant difference in bilateral nasal resistance between cleft subjects (cleft lip, cleft palate, and unilateral cleft lip and palate) and their control group. Thus, in contrast with many other reports in the literature that cleft subjects experience significant nasal obstruction.[6,8–11,22–29,48,50] Drake et al[26] suggested that the cleft nasal passage was about 30% smaller than noncleft nasal passage. Sobol et al[22] reported that children with cleft lip and cleft palate experience nasal obstructive symptoms at a significantly higher rate than unaffected children. Among the different phenotypes of cleft deformities studied by Sobol et al,[22] children with unilateral cleft lip with cleft palate were significantly affected by symptoms of nasal obstruction; those with bilateral cleft lip with palate and those with cleft palate only were not similarly affected. Peroz et al[47] reported correlations between the volume and size of cleft patients' nasal airway and their desire for correction of their nasal function; however, these patients did not report increased severity of nasal obstruction.

In most clinical settings, current standards for evaluating cleft-induced NAO include the patient-reported NOSE questionnaires,[51,52] the facial aesthetic patient-reported outcome instrument (FACE-Q)[53] and the Cleft Evaluation Profile,[54,55] and physical examination maneuvers.[9] These subjective measures are highly dependent on patients' (and/or their primary caregiver) opinions and surgeons' expert opinion. They do not objectively provide physiologic information such as nasal airflow distribution and nasal resistance. These results demonstrate the strong potential of CFD modeling in quantifying nasal patency and our group has been spearheading this effort. We have used CFD modeling to investigate both (1) patient outcomes after NAO in noncleft patients[36,43,56] and (2) the effects of postsurgery maxillary antrostomy size on sinus aeration in patients treated for chronic rhinosinusitis.[32] In another study, using virtually modified nasal cavity models based on a surgeon's edits of presurgery scans to mimic actual surgery done, we evaluated whether such models can accurately predict patients' postoperative nasal outcomes.[41] In Rhee et al,[57,58] we used CFD-based virtual surgery methods to compare computed airflow outcomes from virtual procedures of inferior turbinectomy, septoplasty, and septoplasty with inferior turbinectomy to actual postoperative computed outcomes and to quantify the effects of the following individual virtual procedures on nasal airway patency: nasal valve repair, bilateral inferior turbinectomy, and septoplasty. These findings have provided important information regarding changes in airflow dynamics in the setting of pathology;[32,35,36,43,56] effects of anatomy and nasal disease on topical drug delivery;[33,37,39,40,42,59] and surgical alteration for comparing the contribution of different procedures to nasal function.[34,41,44,60]

CONCLUSIONS

In conclusion, the present study uses computational modeling to provide preliminary objective assessments of the extent of nasal deformity and dysfunction in cleft individuals compared to NAO and normal subjects. Patients with uCLND had significant asymmetry between both sides of the nasal cavity, particularly at the middle-to-posterior region, which is attributable to middle-to-posterior septal deviation. Furthermore, CFD results demonstrate disproportionality in flow partition difference and resistance difference between the cleft and noncleft sides for uCLND patients suggesting that both sides are dysfunctional. Such was not the case for NAO where significantly greater unilateral airflow resistance was reported on the AS (side with septal deviation). Patients with unilateral clefts presenting for treatment of the associated nasal deformity require functional assessment and likely will merit comprehensive functional treatment.

Dennis O. Frank-Ito, PhD
Division of Head and Neck Surgery and
Communication Sciences
Duke University Medical Center
Box 3805
Durham, NC 27710
E-mail: dennis.frank@duke.edu

ACKNOWLEDGMENTS

We give special thanks to ANSYS, Drs. Paolo Maccarini, and Murali Kadiramangalam (ANSYS Global Academic Program Director) for support and strategic donation. All authors gave final approval for publication.

REFERENCES

1. Drettner B. The nasal airway and hearing in patients with cleft palate. *Acta Otolaryngol.* 1960;52:131–142.
2. Hairfield WM, Warren DW, Hinton VA, et al. Inspiratory and expiratory effects of nasal breathing. *Cleft Palate J.* 1987;24:183–189.
3. Hairfield WM, Warren DW, Seaton DL. Prevalence of mouth-breathing in cleft lip and palate. *Cleft Palate J.* 1988;25:135–138.
4. Warren DW, Duany LF, Fischer ND. Nasal pathway resistance in normal and cleft lip and palate subjects. *Cleft Palate J.* 1969;6: 134–140.
5. Warren DW, Drake AF, Davis JU. Nasal airway in breathing and speech. *Cleft Palate Craniofac J.* 1992;29:511–519.
6. Warren DW, Hairfield WM, Dalston ET, et al. Effects of cleft lip and palate on the nasal airway in children. *Arch Otolaryngol Head Neck Surg.* 1988;114:987–992.
7. Marcusson A, Akerlind I, Paulin G. Quality of life in adults with repaired complete cleft lip and palate. *Cleft Palate Craniofac J.* 2001;38:379–385.
8. Massie JP, Runyan CM, Stern MJ, et al. Nasal septal anatomy in skeletally mature patients with cleft lip and palate. *JAMA Facial Plast Surg.* 2016;18:347–353.
9. Fisher MD, Fisher DM, Marcus JR. Correction of the cleft nasal deformity: from infancy to maturity. *Clin Plast Surg.* 2014;41: 283–299.
10. Morén S, Mani M, Lundberg K, et al. Nasal symptoms and clinical findings in adult patients treated for unilateral cleft lip and palate. *J Plast Surg Hand Surg.* 2013;47:383–389.
11. Starbuck JM, Friel MT, Ghoneima A, et al. Nasal airway and septal variation in unilateral and bilateral cleft lip and palate. *Clin Anat.* 2014;27:999–1008.
12. Robison JG, Otteson TD. Increased prevalence of obstructive sleep apnea in patients with cleft palate. *Arch Otolaryngol Head Neck Surg.* 2011;137:269–274.
13. Muntz H, Wilson M, Park A, et al. Sleep disordered breathing and obstructive sleep apnea in the cleft population. *Laryngoscope.* 2008;118:348–353.
14. Maclean JE, Waters K, Fitzsimons D, et al. Screening for obstructive sleep apnea in preschool children with cleft palate. *Cleft Palate Craniofac J.* 2009;46:117–123.
15. Wilson AC, Moore DJ, Moore MH, et al. Late presentation of upper airway obstruction in Pierre Robin sequence. *Arch Dis Child.* 2000;83:435–438.
16. Spier S, Rivlin J, Rowe RD, et al. Sleep in Pierre Robin syndrome. *Chest.* 1986;90:711–715.
17. Marcus CL, Brooks LJ, Ward SD, et al. Diagnosis and management of childhood obstructive sleep apnea syndrome. *Pediatrics.* 2012;130:e714–e55.
18. Li AM, So HK, Au CT, et al. Epidemiology of obstructive sleep apnoea syndrome in Chinese children: a two-phase community study. *Thorax.* 2010;65:991–997.
19. Bixler EO, Vgontzas AN, Lin HM, et al. Sleep disordered breathing in children in a general population sample: prevalence and risk factors. *Sleep.* 2009;32:731–736.
20. O'Brien LM, Holbrook CR, Mervis CB, et al. Sleep and neurobehavioral characteristics of 5- to 7-year-old children with parentally reported symptoms of attention-deficit/hyperactivity disorder. *Pediatrics.* 2003;111:554–563.
21. MacLean JE, Fitzsimons D, Fitzgerald DA, et al. The spectrum of sleep-disordered breathing symptoms and respiratory events in infants with cleft lip and/or palate. *Arch Dis Child.* 2012;97:1058–1063.
22. Sobol DL, Allori AC, Carlson AR, et al. Nasal airway dysfunction in children with cleft lip and cleft palate: results of a cross-sectional population-based study, with anatomical and surgical considerations. *Plast Reconstr Surg.* 2016;138:1275–1285.
23. Latham RA. The pathogenesis of the skeletal deformity associated with unilateral cleft lip and palate. *Cleft Palate J.* 1969;6: 404–414.
24. Crockett D, Bumstead R. Nasal airway, otologic and audiologic problems associated with cleft lip and palate. In: *Multidisciplinary Management of Cleft Lip and Palate.* Philadelphia, Pa.: WB Saunders; 1990.
25. Friel MT, Starbuck JM, Ghoneima AM, et al. Airway obstruction and the unilateral cleft lip and palate deformity: contributions by the bony septum. *Ann Plast Surg.* 2015;75:37–43.
26. Drake AF, Davis JU, Warren DW. Nasal airway size in cleft and noncleft children. *Laryngoscope.* 1993;103:915–917.
27. Farzal Z, Walsh J, Lopes de Rezende Barbosa G, et al. Volumetric nasal cavity analysis in children with unilateral and bilateral cleft lip and palate. *Laryngoscope.* 2016;126:1475–1480.
28. Trindade IE, Gomes Ade O, Fernandes Mde B, et al. Nasal airway dimensions of children with repaired unilateral cleft lip and palate. *Cleft Palate Craniofac J.* 2015;52:512–516.
29. Grossmann N, Brin I, Aizenbud D, et al. Nasal airflow and olfactory function after the repair of cleft palate (with and without cleft lip). *Oral Surg Oral Med Oral Pathol Oral Radiol Endod.* 2005;100:539–544.
30. Cannon DE, Frank DO, Kimbell JS, et al. Modeling nasal physiology changes due to septal perforations. *Otolaryngol Head Neck Surg.* 2013;148:513–518.
31. Cheng T, Carpenter D, Cohen S, et al. Investigating the effects of laryngotracheal stenosis on upper airway aerodynamics. *Laryngoscope.* 2018;128:E141–E149.
32. Frank DO, Zanation AM, Dhandha VH, et al. Quantification of airflow into the maxillary sinuses before and after functional endoscopic sinus surgery. *Int Forum Allergy Rhinol.* 2013;3:834–840.

33. Frank DO, Kimbell JS, Cannon D, et al. Deviated nasal septum hinders intranasal sprays: a computer simulation study. *Rhinology*. 2012;50:311–318.
34. Frank-Ito DO, Sajisevi M, Solares CA, et al. Modeling alterations in sinonasal physiology after skull base surgery. *Am J Rhinol Allergy*. 2015;29:145–150.
35. Choi KJ, Jang DW, Ellison MD, et al. Characterizing airflow profile in the postoperative maxillary sinus by using computational fluid dynamics modeling: a pilot study. *Am J Rhinol Allergy*. 2016;30:29–36.
36. Sullivan CD, Garcia GJ, Frank-Ito DO, et al. Perception of better nasal patency correlates with increased mucosal cooling after surgery for nasal obstruction. *Otolaryngol Head Neck Surg*. 2014; 150:139–147.
37. Frank DO, Kimbell JS, Pawar S, et al. Effects of anatomy and particle size on nasal sprays and nebulizers. *Otolaryngol Head Neck Surg*. 2012;146:313–319.
38. Naftali S, Rosenfeld M, Wolf M, et al. The air-conditioning capacity of the human nose. *Ann Biomed Eng*. 2005;33:545–553.
39. Keeler JA, Patki A, Woodard CR, et al. A computational study of nasal spray deposition pattern in four ethnic groups. *J Aerosol Med Pulm Drug Deliv*. 2016;29:153–166.
40. Frank-Ito, D. O., Wofford, M., Schroeter, J. D., & Kimbell, J. S. (2016). Influence of mesh density on airflow and particle deposition in sinonasal airway modeling. Journal of aerosol medicine and pulmonary drug delivery, 29(1), 46–56.
41. Frank-Ito DO, Kimbell JS, Laud P, et al. Predicting postsurgery nasal physiology with computational modeling: current challenges and limitations. *Otolaryngol Head Neck Surg*. 2014;151: 751–759.
42. Frank DO, Kimbell JS, Cannon D, Rhee JS. Computed intranasal spray penetration: comparisons before and after nasal surgery. *Int Forum Allergy Rhinol*. 2013;3:48–55.
43. Kimbell JS, Frank DO, Laud P, et al. Changes in nasal airflow and heat transfer correlate with symptom improvement after surgery for nasal obstruction. *J Biomech*. 2013;46:2634–2643.
44. Rhee JS, Cannon DE, Frank DO, et al. Role of virtual surgery in preoperative planning: assessing the individual components of functional nasal airway surgery. *Arch Facial Plast Surg*. 2012;14:354–359.
45. Šidlof, P., & Zörner, S. (2013). Computational aeroacoustics of human phonation. In EPJ Web of Conferences (Vol. 45, p. 01085). EDP Sciences.
46. Kim SK, Heo GE, Seo A, et al. Correlation between nasal airflow characteristics and clinical relevance of nasal septal deviation to nasal airway obstruction. *Respir Physiol Neurobiol*. 2014;192:95–101.
47. Peroz R, Holmström M, Mani M. Can objective measurements of the nasal form and function represent the clinical picture in unilateral cleft lip and palate? *J Plast Reconstr Aesthet Surg*. 2017;70:653–658.
48. Shih CW, Sykes JM. Correction of the cleft-lip nasal deformity. *Facial Plast Surg*. 2002;18:253–262.
49. Sandham A, Solow B. Nasal respiratory resistance in cleft lip and palate. *Cleft Palate J*. 1987;24:278–285.
50. Mani M, Morén S, Thorvardsson O, et al. EDITOR'S CHOICE: objective assessment of the nasal airway in unilateral cleft lip and palate–a long-term study. *Cleft Palate Craniofac J*. 2010;47: 217–224.
51. Stewart MG, Witsell DL, Smith TL, et al. Development and validation of the Nasal Obstruction Symptom Evaluation (NOSE) scale. *Otolaryngol Head Neck Surg*. 2004;130:157–163.
52. Stewart MG, Smith TL, Weaver EM, et al. Outcomes after nasal septoplasty: results from the Nasal Obstruction Septoplasty Effectiveness (NOSE) study. *Otolaryngol Head Neck Surg*. 2004; 130:283–290.
53. Klassen AF, Cano SJ, Scott A, et al. Measuring patient-reported outcomes in facial aesthetic patients: development of the FACE-Q. *Facial Plast Surg*. 2010;26:303–309.
54. Turner SR, Thomas PW, Dowell T, et al. Psychological outcomes amongst cleft patients and their families. *Br J Plast Surg*. 1997;50:1–9.
55. Thomas PT, Turner SR, Rumsey N, et al. Satisfaction with facial appearance among subjects affected by a cleft. *Cleft Palate Craniofac J*. 1997;34:226–231.
56. Kimbell JS, Garcia GJ, Frank DO, et al. Computed nasal resistance compared with patient-reported symptoms in surgically treated nasal airway passages: a preliminary report. *Am J Rhinol Allergy*. 2012;26:e94–e98.
57. Rhee JS, Cannon DE, Frank DO, et al. Role of virtual surgery in preoperative planning: assessing the individual components of functional nasal airway surgery. *Arch Facial Plast Surg*. 2012;14:354–359.
58. Rhee JS, Pawar SS, Garcia GJ, et al. Toward personalized nasal surgery using computational fluid dynamics. *Arch Facial Plast Surg*. 2011;13:305–310.
59. Wofford MR, Kimbell JS, Frank-Ito DO, et al. A computational study of functional endoscopic sinus surgery and maxillary sinus drug delivery. *Rhinology*. 2015;53:41–48.
60. Shadfar S, Shockley WW, Fleischman GM, et al. Characterization of postoperative changes in nasal airflow using a cadaveric computational fluid dynamics model: supporting the internal nasal valve. *JAMA Facial Plast Surg*. 2014;16:319–327.
61. Marcus, J. R., Brown, D. A., Carpenter, D., Glener, A., Allori, A., & Frank-Ito, D. (2019). Multimodal characterization of the mature septal deformity and airspace associated with unilateral cleft lip and palate. *Plast Reconstr Surg*. 143(3), 865–873.